

LOW-ENERGY EMITTANCE STUDIES WITH THE NEW SNS ALLISON EMITTANCE SCANNER

M.P. Stockli, W. Blokland, T. Gorlov, B. Han, C. Long, T. Pennisi and S. Assadi,
Spallation Neutron Source, Oak Ridge National Laboratory, Oak Ridge, TN37831, USA.

Abstract

The new SNS Allison emittance scanner measures emittances of 65 kV ion beams over a range of ± 116 mrad. Its versatile control system allows for time-dependent emittance measurements using an external trigger to synchronize with pulsed ion beam systems. After an adjustable initial delay, the system acquires an array of equally delayed beam current measurements, each averaged over a certain time span, where all three time parameters are user selectable. The zero offset of the beam current measurements is determined by averaging a fraction of 1 ms shortly before the start of the ion beam pulse.

This paper discusses the optimization of the angular range. In addition it presents the first results and reports an unresolved artefact. Data are presented on the time evolution of emittance ellipses during 0.8 ms long H⁻ beam pulses emerging from the SNS test LEBT, which is important for loss considerations in the SNS accelerator. Additional data explore the emittance growth observed with increasing beam current and/or increasing RF-power.

INTRODUCTION

The transverse emittance of a particle beam is the four-dimensional distribution of the position coordinates along the two configuration space direction transverse to the propagation direction, and their associated velocity coordinates, which are normally expressed as trajectory angles [1]. Sometimes emittances are given as Volumes V_{xy} or as orthogonal, two-dimensional projections A_x and A_y , which are occupied by a certain fraction of the beam. Most often emittances ϵ are given as semi-axis products of equal-area (χ -volume hyper) ellipse [1,2].

$$V_{xy} = \epsilon_{xy} \cdot \pi^2 \leq \epsilon_x \cdot \epsilon_y \cdot \pi^2 / \chi = A_x \cdot A_y / \chi \quad (1)$$

The equal sign applies for uncorrelated x and y coordinates. The shape dependent form factor χ is about 2. This paper discusses the measurement of the two-dimensional distributions, from which ϵ or A can be derived.

THE ALLISON SCANNER

Figure 1 shows the schematic of the new SNS Allison emittance scanner [3] probing a beam of ions with charge q and energy $q \cdot U$. The indicated ion beam position scan yields the distribution of particles with position x that pass through the narrow entrance slit. At each position, a voltage sweep measures the distribution of trajectory angles x' .

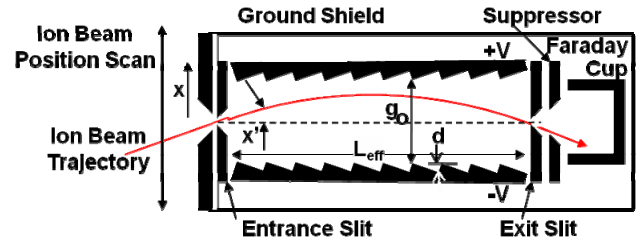


Figure 1: Schematic of SNS Allison Emittance Scanner.

THE OPTIMIZATION OF THE DEFLECTION GAP

The deflector plates are stair-cased to prevent impacting particles from being scattered into the exit slit [4]. The staircase with a depth d increases the electric gap $g_e \approx g_0 + d$, where g_0 is the optical gap between the edges of the stairs. As derived elsewhere [5], particles passing the entrance slits with trajectory angle x' need to be redirected to the exit slits, which requires the following bipolar voltages V :

$$V = \pm 2 \cdot g_e \cdot x' \cdot U / L_{\text{eff}} \quad (2)$$

where L_{eff} is the effective length of the deflector [6].

The maximum voltage V_0 of the bipolar supplies limits the trajectory angle that can be probed to:

$$x'_{\text{max},V} = V_0 \cdot L_{\text{eff}} / (2 \cdot g_e \cdot U) \quad (3)$$

In addition, particles impact on a deflection plate if their entry angle exceeds the geometrical limit of the scanner, $x'_{\text{max},g}$:

$$x'_{\text{max},g} = 2 \cdot g_0 / L_{\text{eff}} \quad (4)$$

For a given voltage limit V_0 and a preferred ion energy $q \cdot U$, the angular acceptance range is optimized by matching these two limits, yielding the optimum optical gap $g_{0,\text{opt}}$:

$$g_{0,\text{opt}} = \frac{1}{2} \left(\sqrt{\frac{V_0^2 \cdot L_{\text{eff}}^2}{U} + d^2} - d \right) \quad (5)$$

For the SNS Allison scanner with $L_{\text{eff}} = 119$ mm, $d = 1$ mm, $V_0 = 1000$ V, and $U = 65$ kV, the optimal optical gap is 6.9 mm. This yields an angular range of $x'_{\text{max},g} = x'_{\text{max},V} = \pm 116$ mrad.

THE UNRESOLVED ARTEFACT

Figure 2 shows the data from an expanding -65 keV H⁻ beam emerging from the SNS LEBT on the test stand.

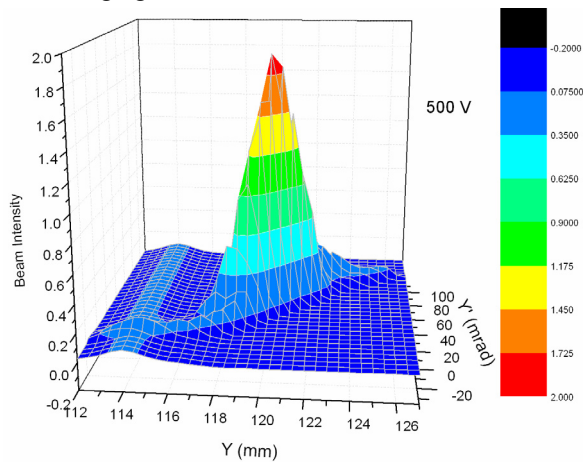


Figure 2: Emittance data of 65 keV H⁻ beam with artefact.

In addition to the negative signals from the H⁻ beam, there are negative signals forming a ridge-shaped artefact centred around 114 mm, or about 6 mm higher than the beam axis. This distance varies significantly for different setups. The false signals only appear when the beam is present. They are not affected by the deflection voltage, which excludes charged particles passing through both sets of slits.

The false signals are not affected by the suppressor voltage, which excludes secondary electrons generated by the neutral beam impacting on the Faraday cup or the exit slit.

Initial attempts to improve the shielding of the Faraday cup cable have failed to reduce the false signals. The efforts to identify the cause of the artefact and to mitigate it continue. In the meantime emittance data are excluded from the analysis if they fall below a threshold equal to 10% of the maximum beam current measured in the specific scan. While a 10% threshold significantly alters the results [7], it is not uncommon at low energies, where the ion beams normally show large tails and strong aberrations. A large threshold enhances the contributions from the core of the beam and therefore can be more meaningful, at least for systems with significantly limited acceptance [2].

SNS LEBT EMITTANCE DATA

Currently the emittance scanner is located ~55 mm from the outlet of the SNS Low-Energy Beam Transport system (LEBT), as shown in the PBGUNS [8] beam transport calculation shown in Fig. 3.

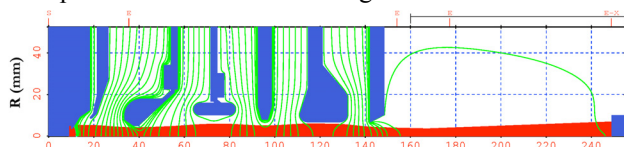


Figure 3: PBGUNS beam transport for an emittance scan.

This large distance makes it impossible to characterize the strongly converging beam injected into the RFQ.

A focus in high-current charged-particle beams can increase its emittance. For this reason, the lenses are operated with smaller voltages than during normal operation on the SNS Front End [8].

Running the e-dump at 5 kV and both lenses at 40 kV yields the emittances shown in Fig. 4. It shows 18 snapshots 50 μs apart, each averaged over 40 μs. The first snapshot shows a random distribution measured before the beam has arrived. A rapid change is found between the 2nd and 3rd snapshot due to changing conditions in the plasma, the meniscus, and space charge neutralization of the beam. The 3rd snapshot is followed by much more gradual changes, except for the last one, when the plasma dies down.

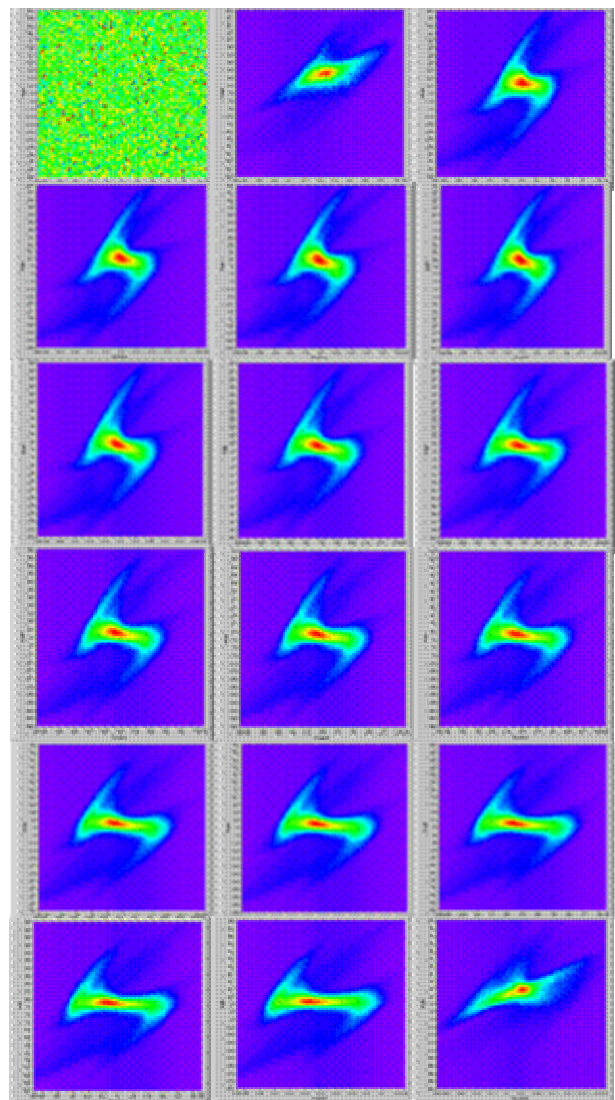


Figure 4: 18 sequential emittance distributions during a 0.8 ms long pulse.

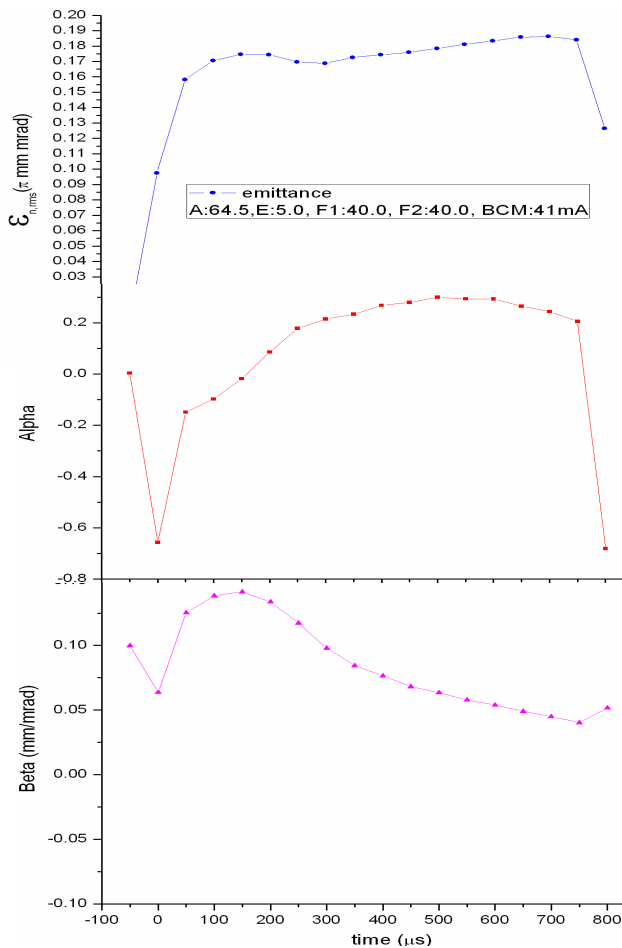


Figure 5: The evolution of the rms emittance and rms Twiss parameters of the 0.8 ms pulse from Fig. 4.

Figure 5 shows the rms emittance to be fairly constant throughout the pulse, except for the smaller emittances of the partial beams at the beginning and the end of the pulse.

Of larger concern are the rms Twiss parameters that gradually change throughout the entire pulse. This confirms earlier observations when tuning the LEBT, which yielded different optimum settings for early in the pulse and at the end of the pulse. So far the problem has been addressed by tuning the LEBT with a part of the beam about halfway through the pulse. However, having a more accurate measure of the effect enables a search for correlations with other parameters, such as the voltage stability of certain electrodes.

Figure 6 shows the normalized rms-emittances as a function of beam current measured near the outlet of the

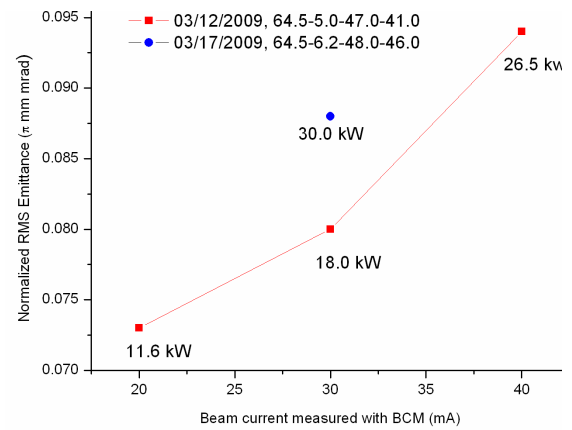


Figure 6: normalized rms-emittances as a function of the LEBT output beam current obtained with the indicated RF power.

LEBT on the test stand. The labels list the 2MHz power that was used to generate the corresponding beam current.

The data show that the emittance depends on the beam current as well as the RF power used to generate the desired beam current. The data which required 30 kW for 30 mA represents an imperfectly cesiated source and therefore follows a different efficiency curve. It is not clear whether the dependence can be factored into a RF power dependence and a beam current dependence.

It is, however, interesting to note that the emittance increases roughly with the square-root of the beam current, which means that the brightness remains roughly the same.

REFERENCES

- [1] Lejeune C., Aubert J., in Applied Charged Particle Optics, Part A, A. Septier ed., Academic Press, New York, 1980, 159-259.
- [2] Stockli M.P., AIP Conf. Proc. 868, Melville, NY, 2006, 25-62.
- [3] Allison P.W., Sherman J.D., and Holtkamp D.B., IEEE Trans. Nucl. Sci. NS-30, 1983, 2204-2206.
- [4] Stockli M.P. et al., AIP CP749, Melville, NY, 2005, 108-111.
- [5] Stockli M.P. et al., AIP CP763, Melville, NY, 2005, 145-158.
- [6] Wollnik H. and Ewald H., Nucl. Instr. Meth. 36, 1965, 93-104.
- [7] Stockli M.P. et al, AIP CP639, Melville, NY, 2002, 135-159.
- [8] Han B. et al., these proceedings.